Hierarchical Bayesian Inference and Learning in Spiking Neural Networks

Shangqi Guo, Zhaofei Yu, Fei Deng, Xiaolin Hu, *Senior Member, IEEE*, and Feng Chen, *Member, IEEE*

***Abstract*—Numerous experimental data from neuroscience and psychological science suggest that human brain utilizes Bayesian principles to deal the complex environment. Furthermore, hierarchical Bayesian inference has been proposed as an appropriate theoretical framework for modeling cortical processing. However, it remains unknown how such a computation is organized in the network of biologically plausible spiking neurons. In this paper, we propose a hierarchical network of winner-take-all circuits which can carry out hierarchical Bayesian inference and learning through a spike-based variational expectation maximization (EM) algorithm. Particularly, we show how the firing activities of spiking neurons in response to the input stimuli and the spike-timing-dependent plasticity rule can be understood, respectively, as variational E-step and M-step of variational EM. Finally, we demonstrate the utility of this spiking neural network on the MNIST benchmark for unsupervised classification of handwritten digits.**

***Index Terms*—Hierarchical Bayesian model, mean field theory, spike-timing-dependent plasticity (STDP), spiking neural network, variational expectation maximization, winner-takes-all (WTA) circuits.**

I. Introduction

THERE is psychophysical and neurophysiological evidence that the brain utilizes Bayesian principles to deal with the complex environment [1]–[3]. Bayesian inference has been suggested as an effective mechanism in various tasks of human brain such as cognition [4], cue combination [5], and decision making [6]. Many electrophysiological experiments verify that the cerebral cortex has a layered structure [7] and the manner of cortical information processing is hierarchical [8]–[10]. These findings lead to propose hierarchical Bayesian inference as a potential computational framework of cerebral cortex [11], [12]. In the real world, living creatures need to handle the environment full of uncertainty and ambiguity. They must have ability to infer the hidden states once given sensory stimuli from the complex environment. These tasks require extracting multiple level abstract features from sensory stimuli and performing inferences at different levels. The hierarchical architectures allow the cortex to extract abstract concepts from inputs layer by layer. Hierarchical Bayesian inference has been proposed to model such process [11], [13], [14]. Furthermore, hierarchical models of cerebral cortex has obtained a remarkable success in the field of deep learning [15]. However, it remains greatly unknown whether hierarchical Bayesian inference and learning could be implemented by biologically plausible spiking neurons and synaptic plasticity rules. Bridging this gap between hierarchical Bayesian model and spiking neural network is of great importance, since it can help us understand the Bayesian process of human brain.

Recently, a variety of spiking neural circuits have been proposed to deal with different Bayesian models, and they can be roughly divided into two categories. One of them focuses only on the inference problem. For instance, Rao [16] linked the firing-rate dynamics of recurrent spiking neural network to belief propagation equation for hidden Markov model. Buesing *et al.* [17] and Pecevski *et al.* [18] proposed a recurrent network of spiking neurons to perform probabilistic inference via Markov chain Monte Carlo sampling. Shi and Griffiths [13] designed a rate-based neural circuit to implement chain-like Bayesian inference via importance sampling. Ma *et al.* [19] proposed that populations of neurons could represent probability distributions and perform Bayesian inference through a linear combination of populations of neurons. The other category performs both inference and learning. Huang and Rao [20] proposed a two-layer recurrent network of Poisson neurons to perform both approximate Bayesian inference and learning for any hidden Markov model. Sountsov and Miller [21] designed a spiking neuronal network to implement the local delta learning rule for two-layer Helmholtz machine. Nessler *et al.* [22] showed that a winner-take-all (WTA) circuit with the spike-timing-dependent plasticity (STDP) learning rule can perform an online expectation maximization (EM) algorithm for mixtures of Bernoulli distributions, which is called spike-based EM algorithm. Based on this algorithm, Pecevski and Maass [23]

Manuscript received April 13, 2017; revised September 9, 2017; accepted October 22, 2017. This work was supported in part by the National Natural Science Foundation of China under Grant 61671266, Grant 61327902, and Grant 91420201, in part by the Research Project of Tsinghua University under Grant 20161080084, in part by the National High-Tech Research and Development Plan under Grant 2015AA042306, in part by the Beijing Municipal Science and Technology Commission under Grant Z161100000216126, and in part by the Huawei Technology under Contract YB2015120018. This paper was recommended by Associate Editor Y. Xiang. *(Shangqi Guo and Zhaofei Yu contributed equally to this work.) (Corresponding authors: Xiaolin Hu; Feng Chen.)*

S. Guo, Z. Yu, F. Deng, and F. Chen are with the Department of Automation, Tsinghua University, Beijing 100086, China, and also with the LSBDPA Beijing Key Laboratory, Beijing 100084, China (e-mail: gsq15@mails.tsinghua.edu.cn; yuzf12@mails.tsinghua.edu.cn; dengf15@mails.tsinghua.edu.cn; chenfeng@tsinghua.edu.cn).

X. Hu is with the Department of Computer Science and Technology, TNLIST, Center for Brain-Inspired Computing Research, Tsinghua University, Beijing 100084, China (e-mail: xlhu@mail.tsinghua.edu.cn).

Color versions of one or more of the figures in this paper are available online at http://ieeexplore.ieee.org.

Digital Object Identifier 10.1109/TCYB.2017.2768554

proposed to combine such network motifs recursively into a neural circuit that can perform learning of Bayesian networks.

Nevertheless, it is difficult to extend these spiking neural networks to implement inference and learning for Bayesian models with hierarchical structures. Consequently, there is a gap between hierarchical Bayesian models and biologically plausible networks of spiking neurons. To bridge the gap, we propose a hierarchical network of WTA circuits (hierarchical-WTA) which can implement representation, inference and learning of hierarchical Bayesian models with tree structures. The hierarchical-WTA is based on the idea that combinations of WTA circuits can perform mean field inference. The mean field theory utilizes a fully factorized model to approximate a complex Bayesian model. Thus, this idea can be interpreted as a tradeoff between local computation and global computation. Although we mainly focus on tree-structured models, the neural implementation of such models can extend to arbitrary Bayesian networks by merging variables.

Importantly, we interpret the computational role of the hierarchical-WTA as a spike-based variational EM algorithm. This algorithm consists of two procedures: 1) spike-based variational E-step and 2) spike-based variational M-step. For the spike-based variational E-step, we will show how the dynamic firing responses of hierarchical-WTA can be viewed as mean field equations to optimize the Kullback–Leibler divergence between the exact posterior probability and the mean field distribution. In other words, the hierarchical-WTA can implement mean field equations via discrete action potentials. This procedure not only reduces global computation to local computation but also provides a lower bound for variational Bayesian learning. For the spike-based variational M-step, we prove that STDP learning rule can stochastically converge to the set of maxima of the lower bound. To validate the spike-based variational EM algorithm, we test the hierarchical-WTA for unsupervised classification tasks of MNIST dataset.

The organization of this paper is as follows. In Section II, we introduce the definition of the hierarchical-WTA and show how to represent and update hierarchical Bayesian models with the hierarchical-WTA. In Section III, we will develop a theoretical framework for the spike-based variational EM algorithm including mean-field E-step with dynamic firing equations and variational M-step through STDP learning rule. In Section IV, we present the results on the classification task for the MNIST benchmark. Finally, we will give our conclusion and discussion about future researches in Section V.

II. Hierarchical Spiking Neural Network

Hierarchical inference has been suggested as a computational framework to model the cerebral cortex. Building a successful model within this framework helps us to understand how cortical circuits can perform hierarchical processing of sensory stimuli. In this section, we introduce a hierarchical spiking neural network which is called hierarchical-WTA and organized by a group of WTA circuits. This network can represent tree-structured Bayesian models through population code. To enable the hierarchical-WTA to implement inference and learning for the Bayesian model, we will link dynamic firing activities of the hierarchical-WTA and STDP rule to variational EM algorithm. Furthermore, our hierarchical WTA can extend to any hierarchical Bayesian models through combining some variables [24].

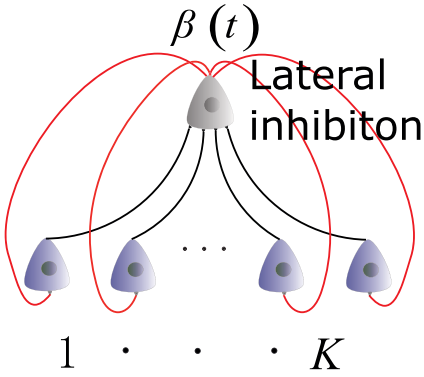

Fig. 1. WTA circuit composed of K excitatory neurons.

A. Hierarchical Network of WTA Circuits

Throughout this paper, we first introduce WTA circuits. WTA circuit is a fundamental building block of cortical microcircuits [25]. In our theoretical framework, there are two important roles that the WTA circuit plays. One of the roles is encoding random variables of Bayesian models via population code and the other role is implementing approximate inference for Bayesian models.

1) WTA Circuit: WTA circuit consists of a population of excitatory neurons and a global inhibitory neuron, as illustrated in Fig. 1. The inhibitory neuron receives input from excitatory neurons via excitatory connections (black synapses) and provides an inhibitory feedback signal fed to all the excitatory neurons. In this paper, we model the circuit in a stochastic way [22], [26]. The excitatory neurons fire a spike with an instantaneous probability. This firing probability depends exponentially on the membrane potential, which has been in accordance with biological findings [27]. The inhibitory neuron installs competition between the excitatory neurons and ensures that overall spiking rate $\hat{\rho}$ of the WTA circuit stays approximately constant. Without loss of generality, we assume $\hat{\rho} = 1$ for the following theoretical analysis. Thus the firing probability of each excitatory neuron k at time t is defined by

$$\rho_k(t) = \hat{\rho} \cdot e^{u_k(t) - \beta(t)} \tag{1}$$

where $u_k(t)$ denotes the membrane potential of neuron k at time t and $\beta(t)$ denotes the inhibitory feedback signal

$$\beta(t) = \sum_{i=1}^{K} e^{u_i(t)}.$$

The excitatory neurons in the WTA circuits are modeled by the spike response model [27], which is a generalization of the leaky integrate-and-fire model and has been shown to match biological data quite well [27]. In the framework of the spike response model, the membrane potential of each neuron k is computed as a summation of excitatory inputs from the presynaptic neurons $pre(k)$ through synaptic weights

TABLE I
DEFINITIONS OF THE MAIN MATHEMATICAL SYMBOLS USED IN THIS PAPER

Variables and parameters in the model of WTA circuit	
$u_k(t)$	the membrane potential of neuron k at time t
$\hat{\rho}$	the overall firing rate of WTA circuits
$\beta(t)$	the feedback inhibitory signal
$\kappa(t)$	the excitatory postsynaptic potentials (EPSP) kernel
$\Theta(t)$	Heaviside step function
$S_i(t)$	the spike train of the neuron i
t_i^f	the firing time of the f-th spike of the neuron i
Variables and parameters in the underlying Bayesian model	
$\mathbf{z_v}$	vector of all visible variables $\{z_1, ..., z_v\}$
$\mathbf{z_h}$	vector of all hidden variables $\{z_{v+1}, ..., z_{R+1}\}$
$\mathbf{w}$	vector of all synaptic weights $\left\{w_l^{ij}, l \le R, i \le K, j \le K\right\}$
$p^*(\mathbf{z_v})$	the actual input distribution
$z_{pa(l)}$	the parent node of z_l
$z_{ch(l)}$	the children nodes of z_l
Variables and parameters in the hierarchical-WTA	
G_l	the l-th WTA circuit that encodes the variable z_l
z_l^k	the k-th excitatory neurons of G_l that encodes $z_l = k$
w_l^{ij}	the synaptic weights between G_l and $G_{pa(l)}$
$S_l^k(t)$	the spike train of the neuron z_l^k
$u_l^k(t)$	the membrane potential of the neuron z_l^k at time t
$\rho_l^k(t)$	the firing probability of the neuron z_l^k at time t
Variables and parameters in the process of STDP learning	
$\triangle w_l^{ij}$	the change of the synaptic weight w_l^{ij}
$W(s)$	the learning window of the long term potentiation part
A_w	the amplitude parameter of the learning window
a	the constant contribution for the long term depression
ξ_l^j	adaptive learning rate of the synaptic w_l^{ij}

$w_{ik}(i \in \text{pre}(k))$. The excitatory postsynaptic potentials (EPSPs) kernel $\kappa(t)$ describes the electrical properties of the membrane after spiking neurons receive an action potential. In this paper, we use a biologically realistic alpha shaped EPSP (any other EPSP shapes can be extended without efforts in our theoretical model) defined by

$$\kappa(t) = \kappa_0 \cdot \left(\exp\left(-\frac{t}{\tau_f}\right) - \exp\left(-\frac{t}{\tau_s}\right)\right) \cdot \Theta(t) \tag{2}$$

where $\tau_f = 2$ ms and $\tau_s = 8$ ms, respectively, denotes fast time constant and slow time constant. $\kappa_0 = [1/(\hat{p} \cdot (\tau_f - \tau_s))]$ denotes amplitude of EPSP kernel. Introducing the spike train $S_i(t) = \sum_f \delta(t - t_i^f)$ of the neuron i, where t_i^f denotes the firing time of the fth spike of the neuron i. Then the membrane potential $u_k(t)$ of the neuron k is given by

$$u_k(t) = \sum_{i \in \text{pre}(k)} w_{ik} \cdot \int_0^\infty \kappa(s) S_i(t-s) ds \tag{3}$$

where w_{ik} denotes the synaptic weight between presynaptic neuron i and neuron k. We summarize the important mathematical notations in Table I.

2) Definition of the Hierarchical-WTA: The hierarchical-WTA is a hierarchical network consisting of a group of WTA circuits. We assume that every circuit is composed of K excitatory neurons (one can choose any size for the circuit). To clarify the distinction between these circuits, we denote each WTA circuit by $G_l(l = 1, \ldots, R+1)$ and use $z_l^k(k = 1, \ldots, K)$ to denote each excitatory neuron of the circuit G_l. The circuit G_{R+1} at the root node represents the output of the hierarchical-WTA and the circuits $G_1, \ldots, G_v$ at the bottom layer are used to receive external inputs. The hierarchical-WTA has the structural constraint that WTA circuits are organized in the rooted tree structure, as illustrated in Fig. 2(a). Under the structural constraint, each WTA circuit $G_l(l = 1, \ldots R)$ just connects one WTA circuit at the upper layer [i.e., the parent node $pa(l)$] and a number of WTA circuits at the lower layer [i.e., the children nodes $ch(l)$]. The synaptic connections between WTA circuits are fully connected and bidirectional. In the following, we use $w_l^{ij}(i = 1, \ldots, K, j = 1, \ldots, K)$ to denote the synaptic efficacies between the WTA circuit G_l and the WTA circuit $G_{pa(l)}$ at the parent node.

In our computational framework, the hierarchical-WTA can be used to implement three fundamental features of a Bayesian model: 1) representation; 2) inference; and 3) learning. WTA circuits are used to encode any discrete random variable by population code and the synaptic connections between WTA circuits encode the conditional independencies among these random variables. Hence, one can combine WTA circuits to represent any tree-structure Bayesian model over discrete random variables. The inference task of the underlying Bayesian model can be implemented through the dynamic activities of the hierarchical-WTA network. The learning goal is to find synaptic weights, such that the marginal distribution of the underlying Bayesian model approximates the actual distribution of external inputs as closely as possible. This is performed through the STDP learning rule.

B. Underlying Bayesian Model

From the perspective of probabilistic graphical model, our hierarchical-WTA circuit is interpreted as a Bayesian generative model with a hierarchical tree structure as shown in Fig. 2(b). This generative model is represented by a distribution $p(\mathbf{z}|\mathbf{w})$ over discrete random variables $z_1, \ldots, z_{R+1}$, where $\mathbf{w}$ denote the collection of synaptic weights. The random variables $z_1, \ldots, z_{R+1}$ can be divided into two types, visible variables and hidden variables. The visible variables are represented by the WTA circuits at the bottom layer of the hierarchical-WTA and the hidden variables are represented by the WTA circuits at the hidden layers of hierarchical-WTA. For the convenience, we denote the visible variables collection by $\mathbf{z_v} = \{z_1, \ldots, z_v\}$ and the hidden variables collection by $\mathbf{z_h} = \{z_{v+1}, \ldots, z_{R+1}\}$.

In order to encode the Bayesian model, we use the following method. Every random variable z_l is encoded by the WTA circuit G_l and the conditional probability $p(z_l|z_{pa(l)})$ is encoded by the synaptic connections $w_l^{ij}(i = 1, \ldots, , K, j = 1, \ldots, K)$. We first introduce population coding to represent the random variable z_l by the excitatory neurons $z_l^k(k = 1, \ldots, K)$ installed in the WTA circuit G_l. It also applies to the other variables. For every possible value of the variable z_l, there is exactly one neuron of the population neurons $z_l^k(k = 1, \ldots, K)$ to encode it. We use the spike train $S_l^k(t)$ from the neuron z_l^k to represent the instantaneous value k of the variable z_l at the time t of the spike

$$S_l^k(t) = 1 \Leftrightarrow z_l = k. \tag{4}$$

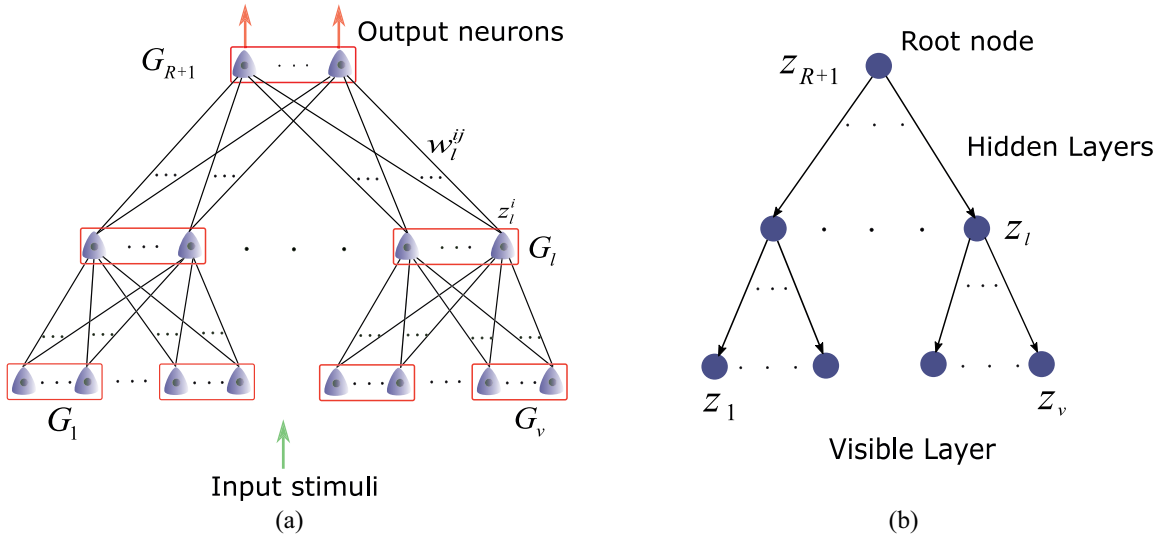

Fig. 2. (a) Three-layer hierarchial-WTA network. (b) Underlying hierarchical Bayesian model with tree structure.

In this way, every neuron $z_l^k (k = 1, \ldots, K)$ of the WTA circuit G_l represents one of K possible values for the random variable z_l.

Then we use the synaptic weights $w_l^{ij} (i = 1, \ldots, K, j = 1, \ldots K)$ between the WTA circuit G_l and the WTA circuit $G_{pa(l)}$ to encode the conditional probabilities $p(z_l|z_{pa(l)})$

$$w_l^{ij} = \log p\big(z_l = i|z_{pa(l)} = j\big) + \hat{w} \tag{5}$$

where $\hat{w}$ denotes the constant which shifts the values for the weights into the positive interval. For the sake of simplicity, we assume that $\hat{w} = 0$ in the following theoretical analysis. And we set $\hat{w} = 5$ in the simulation.

Thus we can formulate the hierarchical-WTA by the joint probabilistic distribution $p(\mathbf{z_h}, \mathbf{z_v}|\mathbf{w})$

$$\begin{aligned} p(\mathbf{z_h}, \mathbf{z_v}|\mathbf{w}) &= p(z_{R+1}) \prod_{l=1}^{R} p\big(z_l|z_{pa(l)}, \mathbf{w}\big) \\ &= p(z_{R+1}) \prod_{l=1}^{R} \prod_{j=1}^{K} \big(p\big(z_l|z_{pa(l)} = j, \mathbf{w}\big)\big)^{\delta(z_{pa(l)}=j)} \\ &= p(z_{R+1}) \prod_{l=1}^{R} \prod_{j=1}^{K} \left(\frac{1}{Z_l^j} \prod_{i=1}^{K} \left(e^{w_l^{ij}}\right)^{\delta(z_l=i)}\right)^{\delta(z_{pa(l)}=j)} \end{aligned} \tag{6}$$

where $\delta(\cdot)$ is the Dirac delta function. Z_l^j denotes the normalization constant

$$Z_l^j = \sum_{i=1}^{K} e^{w_l^{ij}}. \tag{7}$$

We assume that all possible states of the root node z_{R+1} have the same prior, i.e., uniform distribution. As can be seen, the visible variables are conditionally independent given the hidden variables. This strong assumption can be relaxed by a tree-structured model [28], [29].

Although the underlying Bayesian model is a tree-structure model, there are two reasons to study this kind of model.

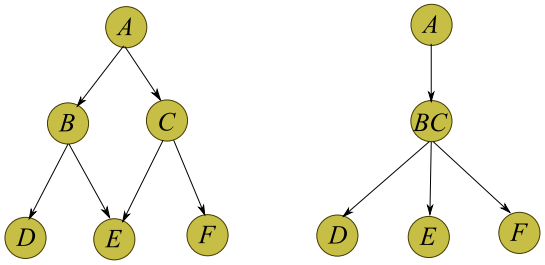

Fig. 3. Bayesian network (left) and a corresponding tree-structured network (right).

First, arbitrary Bayesian model can be converted to a tree-structure model [24] by combining some variables together. For instance, in Fig. 3, we can convert the left Bayesian network to a tree-structured Bayesian network by clustering B and C into a single variable BC. Thus the neural implementation of tree-structure Bayesian models can be extended to arbitrary Bayesian models. Second, tree-like topological structures reflect a hierarchical part-based group of the visible variables and have been explored in a variety of domains [30], [31].

C. Dynamic Firing Equation

For the underlying Bayesian model, the inference and learning problem can be performed via EM algorithm [32]. In the E-step of the algorithm, one need to evaluate the posterior probability $p(\mathbf{z_h}|\mathbf{z_v}, \mathbf{w})$ over the hidden variables $\mathbf{z_h}$

$$p(\mathbf{z_h}|\mathbf{z_v}, \mathbf{w}) = \frac{p(\mathbf{z_h}, \mathbf{z_v}, \mathbf{w})}{p(\mathbf{z_v}, \mathbf{w})}$$

where

$$p(\mathbf{z_v}, \mathbf{w}) = \sum_{\mathbf{z_h}} p(\mathbf{z_h}, \mathbf{z_v}, \mathbf{w})$$

is the likelihood of the evidence variables. However, the calculation of $p(\mathbf{z_v}, \mathbf{w})$ is global and intractable for the Bayesian network with many hidden variables. Actually, this term can

be computed by summing over all configuration of the hidden variables. If the Bayesian model has N hidden variables and each hidden variable has K possible values, the number of all configuration is K^N. Unfortunately, the calculation of this term is intractable for the hierarchical Bayesian network with many hidden variables. It presents a major obstacle to perform the exact posterior probability inference through local operations of spiking neural networks. Nessler *et al.* [22] mainly focused on for the simple Bayesian models that just have one hidden variable and construct a WTA circuit to evaluate the exact posterior probability. Thus, their algorithm is difficult to generalized to hierarchical Bayesian models with more hidden variables. Our hierarchical-WTA can break the obstacle by variational method. It is based on the idea that combinations of WTA circuits can perform variational mean field inference. The mean field theory is used to convert the difficult problem of exact inference into an easier optimization problem and utilizes a fully factorized model to approximate any Bayesian model.

In the hierarchical-WTA [see Fig. 2(b)], the WTA circuits at the bottom layer are used to encode the input stimuli and the WTA circuits at the hidden layers are in response to the input stimuli. In the bottom layer, each neuron $z_l^k (l = 1, \ldots v, k = 1, \ldots, K)$ will be set to fire at the rate $\hat{\rho}$ and the other neurons in the WTA circuit G_l are inhibited, if the variable $z_l (l = 1, \ldots, v)$ adopts the value k. In the hidden layers, each neuron $z_l^k (l > v,\ k = 1, \ldots, K)$ receives inputs from the neurons of the WTA circuits $G_{ch(l)}$ and the neurons of the WTA circuit $G_{pa(l)}$ (the neurons at the top layer just receive input from WTA circuits at the children nodes). According to (1) and (3), the firing probability $\rho_l^j(t)$ of the neuron $z_l^k (l > v,\ k = 1, \ldots, K)$ at time t can be described by

$$\rho_l^j(t) = \frac{\exp\left(u_l^j(t)\right)}{\sum_j \exp\left(u_l^j(t)\right)}$$

$$u_l^j(t) = b_l^j + \sum_{c \in ch(l)} \sum_{i=1}^{K} w_c^{ij} \cdot I_c^i(t) + \sum_k w_l^{jk} \cdot I_{pa(l)}^k(t) \quad (8)$$

where $u_l^j(t)$ denotes the membrane potential of the neuron z_l^j at time t. $I_c^i(t)(c < R+1, i = 1, \ldots, K)$ represents the input current from the neuron z_c^i. $I_{pa(l)}^k(t)(l < R+1, i = 1, \ldots, K)$ represents the input current from the neuron $z_{pa(l)}^k$

$$I_c^i(t) = \int_0^\infty \kappa(s) S_c^i(t-s) ds \quad (9)$$

$$I_{pa(l)}^k(t) = \int_0^\infty \kappa(s) S_{pa(l)}^k(t-s) ds. \quad (10)$$

In this paper, (8) is called dynamic firing equations. It can be interpreted from the perspective of variational inference. We will prove that the dynamic equations can optimize the Kullback–Leibler divergence between the posterior probability $p(\mathbf{z_h}|\mathbf{z_v}, \mathbf{w})$ and a mean field distribution. In other words, the dynamic firing equations are equivalent to performing mean field inference for the posterior probability. Further theoretical details can be found in Section III-B. This theoretical result gives rise to a new perspective of the computational function of WTA circuits: mean field approximate inference based on spike events.

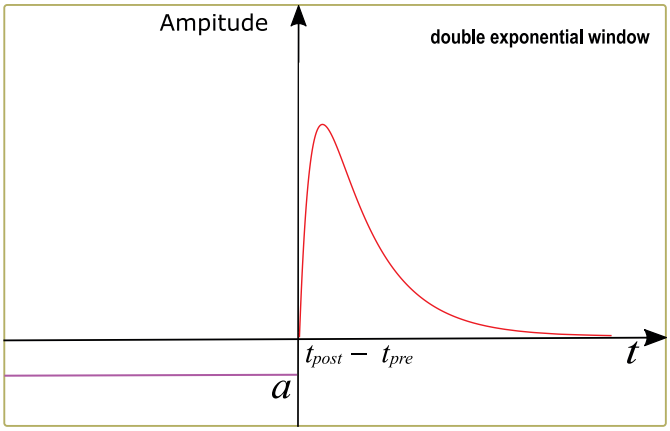

Fig. 4. STDP learning curve.

D. STDP Learning Rules

The learning problem of the hierarchical-WTA is to find synaptic weights $\mathbf{w}$, such that the marginal distribution $p(\mathbf{z_v}|\mathbf{w})$ approximates the actual distribution of inputs $p^*(\mathbf{z_v})$ as closely as possible. Our hierarchical-WTA can accomplish this learning task through the local STDP rule on synaptic connections without supervision.

STDP learning rule is the function of the time difference between presynaptic and postsynaptic spike events, and consists of two-phase learning procedures: 1) long-term potentiation (LTP) and 2) long-term depression (LTD). We choose a variant of the synaptic plasticity form [27] as our STDP learning rule. The STDP learning curves are shown in Fig. 4. The LTP occurs when the presynaptic neuron fires shortly before the postsynaptic spike and the LTD occurs when the postsynaptic neuron fires (see Fig. 4). According to this, the change of the synaptic weight w_l^{ij} is given by

$$\triangle w_l^{ij} = S_{pa(l)}^j(t) \left[a + A_w \int_0^\infty W(s) \cdot S_l^i(t-s) ds \right] \quad (11)$$

$$\text{with} \int_0^\infty W(s) ds = 1 \quad (12)$$

where the contribution for LTD is a constant $a = 1$ and the time dependence for LTP is described by a learning window W with the amplitude parameter $A_w = e^{-(w-\hat{w})}$. Here we introduce a biologically realistic double-exponential window

$$W(t) = \frac{1}{\tau_f - \tau_s} \left(\exp\left(-\frac{t}{\tau_f}\right) - \exp\left(-\frac{t}{\tau_s}\right) \right) \cdot \Theta(t) \quad (13)$$

where fast and slow time constants are set to $\tau_f = 2$ ms and $\tau_s = 8$ ms.

Applying the STDP rule, the synaptic weight w_l^{ij} change according to

$$w_l^{ij} \leftarrow w_l^{ij} + \xi_l^j \cdot \triangle w_l^{ij} \quad (14)$$

where we use a adaptive learning rate $\xi_l^j = (1/N_l^j)$ with N_l^j representing the total number of the postsynaptic spikes.

In this paper, we exploit a computational property of STDP in the hierarchical-WTA network: the STDP learning rule (11) drives the synaptic weights in the hierarchical network to converge stochastically to the set of maxima of the lower bound of the data log-likelihood. Further theoretical details can be found in Section III-C. The plasticity rule is similar to the synaptic weight update which is emerged as parameters learning for EM algorithm, in related studies [22], [26]. However, the STDP rule installed in our hierarchical networks is viewed as variational M-step of the variational EM algorithm which can be applied to more complex Bayesian model.

III. Spike-Based Variational Expectation Maximization Algorithm

Human brain can perform fast computations with ease spiking neurons and local computational operations. However, Bayesian inference for the hierarchical Bayesian network with many hidden variables is computationally intractable and global. This computational complexity result seems to be in strong contrast with human brain. To break the obstacle, we utilize variational principle to handle the difficult problem of exact inference by converting it into an easier optimization problem, which has been discussed and suggested in the neuroscience literatures [12]. With the variational principle, we develop a spike-based variational EM algorithm. As far as we known, such a framework has not been considered in the other works. In the following, we will show two key theoretical results.

1) The dynamic firing equations (8) are equivalent to the mean field equations (22).
2) The STDP rule (11) stochastically converges to the set of maxima of the lower bound of the log-likelihood.

A. Goal of the Network Optimization

The goal of the hierarchical-WTA optimization is to minimize the error between the model marginal likelihood $p(\mathbf{z_v}|\mathbf{w})$ and the actual distribution of the inputs denoted by $p*(\mathbf{z_v})$. A natural measurement of the error is the Kullback–Leibler divergence

$$KL\big(p^*(\mathbf{z_v})\|p(\mathbf{z_v}|\mathbf{w})\big) = \sum_{\mathbf{z_v}} p^*(\mathbf{z_v}) \log \frac{p^*(\mathbf{z_v})}{p(\mathbf{z_v}|\mathbf{w})} = -\mathbf{H}_{p^*}[\mathbf{z_v}] - L(\mathbf{w}) \tag{15}$$

where $\mathbf{H}_{p^*}[\mathbf{z_v}]$ denotes the entropy of the distribution $p^*(\mathbf{z_v})$ and p^* is the shorthand of $p^*(\mathbf{z_v})$

Since $\mathbf{H}_{p^*}[\mathbf{z_v}]$ is a constant in term of network parameters $\mathbf{w}$, the Kullback–Leibler divergence (15) is equivalent to maximizing the expected log-likelihood

$$L(\mathbf{w}) = \langle \log p(\mathbf{z_v}|\mathbf{w}) \rangle_{p^*} = \left\langle \log \sum_{\mathbf{z_h}} p(\mathbf{z_v}, \mathbf{z_h}|\mathbf{w}) \right\rangle_{p^*} \tag{16}$$

where $\langle\cdot\rangle_{p^*}$ denotes an expectation with respect to $p^*(\mathbf{z_v})$.

This objective function requires to evaluate the posterior probability, but it is often intractable. We therefore resort to the approximation method to perform this computation. In particular, we introduce a variational distribution $Q(\mathbf{z_h}|\varphi)$ to approximate the exact posterior probability. It also provides a lower bound on the likelihood required for learning, which has been proposed to perform variational EM algorithm for generative models [24]

$$\begin{aligned} L(\mathbf{w}) &= \langle \log p(\mathbf{z_v}|\mathbf{w}) \rangle_{p^*} \\ &\geq \langle \log p(\mathbf{z_v}|\mathbf{w}) \rangle_{p^*} - \langle KL(Q(\mathbf{z_h}|\varphi), p(\mathbf{z_h}|\mathbf{z_v}, \mathbf{w})) \rangle_{p^*} \\ &= \big\langle E_Q\big[\log p(\mathbf{z}|\mathbf{w})\big] + \mathbf{H}[Q(\mathbf{z_h}|\varphi)] \big\rangle_{p^*} \\ &= \langle F(Q, \mathbf{w}) \rangle_{p^*} \end{aligned} \tag{17}$$

where $F(Q, \mathbf{w})$ denotes the lower bound of $L(\mathbf{w})$.

The term $\log p(\mathbf{z_v}|\mathbf{w})$ is independent of φ, thus maximizing the lower bound $F(Q, \mathbf{w})$ is equivalent to minimize the KL divergence $KL(Q(\mathbf{z_h}|\varphi), p(\mathbf{z_h}|\mathbf{z_v}, \mathbf{w}))$. Therefore, the problem of approximate inference is cast to the optimization of lower bound with respect to the variational parameters φ. In the following, we will explain how the hierarchical-WTA implements variational EM algorithm to optimize the lower bound. It consists of two steps.

1) *Variational Expectation Step:* Maximizing $F(Q, \mathbf{w})$ with respect to Q through the dynamic firing equation (8).
2) *Variational Maximization Step:* Maximizing $F(Q, \mathbf{w})$ with respect to $\mathbf{w}$ through the STDP learning rule (11).

B. Variational Inference With Dynamic Firing Equation

The bound in (17) is valid for any probability distribution $Q(\mathbf{z_h})$. In probability theory, the mean field theory [33] provides a tractable and simple approximate inference for the exact posterior probability. It is based on a fully factorized distribution $Q(\mathbf{z_h}|\varphi)$ defining over the binary variables $\mathbf{z_h}$ for hidden variables

$$Q\left(\mathbf{z_h}|\varphi) = \prod_{l\in\mathbf{h}} q_l(\mathbf{z}_l|\varphi_l\right) = \prod_{l\in\mathbf{h}}\prod_{i=1}^{K} \big(\varphi_l^i\big)^{z_l^i} \tag{18}$$

where the variational parameters satisfy the normalization condition

$$\forall l : \sum_{i=1}^{K} \varphi_l^i = 1. \tag{19}$$

Then the lower bound $F(Q, \mathbf{w})$ can be written as

$$\begin{aligned} F(Q, \mathbf{w}) &= E_Q\big[\log p(\mathbf{z}|\mathbf{w})\big] + H[Q(\mathbf{z_h}|\varphi)] \\ &= \sum_{l,i,j} E_Q\big[\delta\big(z_{pa(l)} = j\big) \cdot \delta(z_l = i)\big] \cdot w_l^{ij} \\ &\quad - \sum_{l,j} E_Q\big[\delta\big(z_{pa(l)} = j\big)\big] \cdot Z_l^j - \sum_{i,l} \varphi_l^i \cdot \log \varphi_l^i \\ &= \sum_{l,i,j} \varphi_{pa(l)}^j \cdot \varphi_l^i \cdot w_l^{ij} - \sum_{l,j} \varphi_{pa(l)}^j \cdot Z_l^j - \sum_{l,i} \varphi_l^i \cdot \log \varphi_l^i. \end{aligned} \tag{20}$$

When dealing with this formula, we only need to reason about the variables which share a factor with the terms in the Markov blanket and the other terms can be absorbed into the constant term. In the tree-structure Bayesian model, the Markov blanket of each variable z_l consists of parent variable $z_{pa(l)}$ and its children variables $z_{ch(l)}$. If we write the lower

bound with respect to the term involving $q_l(z_l)$ and regard all the other terms as constant, we can get

$$\begin{aligned} F(Q,\mathbf{w}) &= E_Q\big[\log p(\mathbf{z}|\mathbf{w})\big] + H[Q(\mathbf{z_h}|\varphi)] \\ &= \sum_{c\in ch(l)}\sum_{i,j}\varphi_c^i\cdot\varphi_l^j\cdot w_c^{ij} + \sum_{j,k}\varphi_l^j\cdot\varphi_{pa(l)}^k\cdot w_l^{jk} \\ &\quad - \sum_j \varphi_l^j\cdot\log\varphi_l^j - \sum_j\varphi_l^j\cdot\sum_{c\in ch(l)}\log Z_c^j + C(q_l). \end{aligned} \tag{21}$$

Setting the gradient $\partial F(Q,\mathbf{w})/\partial\varphi_l^j$ equal to zero, we will get the mean field update equation

$$\begin{aligned} &\frac{\partial F(Q,\mathbf{w})}{\partial\varphi_l^j} = \sum_{c\in ch(l)}\sum_i\varphi_c^i\cdot w_c^{ij} + \sum_k\varphi_{pa(l)}^k\cdot w_l^{jk} - \log\varphi_l^j \\ &- \sum_{c\in ch(l)}\log Z_c^j = 0 \\ &\Longleftrightarrow \varphi_l^j \propto \exp\left(b_l^j + \sum_{c\in ch(l)}\sum_i\varphi_c^i\cdot w_c^{ij} + \sum_k\varphi_{pa(l)}^k\cdot w_l^{jk}\right) \end{aligned} \tag{22}$$

where

$$b_l^j = -\sum_{c\in ch(l)}\log Z_c^j = -\sum_{c\in ch(l)}\sum_{i=1}^{K_c} e^{w_c^{ij}}.$$

This dynamic equation amounts to performing coordinate ascents of the KL divergence $KL(Q(\mathbf{z_h}|\varphi), p(\mathbf{z_h}|\mathbf{z_v},\mathbf{w}))$. It is a particular set of recursions to find a stationary point and converges to a local optimum of the variational inference problem [33]. In practice, it has been found to converge fairly quickly and to scale well to large-scale networks.

Comparing (22) with (8), there are two critical points to link the mean field inference and the dynamic firing equations of hierarchical-WTA

$$\text{for } l,j: b_l^j = \text{constant and } I_l^j(t) \text{ encodes } \varphi_l^j(t).$$

First of all, the term b_l^j can be viewed as intrinsic excitability of spiking neuron. The calculation of this term involves presynaptic weights, while it is unclear how biologically realistic neurons communicate ongoing changes in synaptic weights from distal synaptic sites to the soma. The STDP learning rules (11) can guarantee that the term b_l^j remains approximately constant. We will prove it in Corollary 1. Second, (22) depends on continuous variational parameters φ, while biologically plausible neurons communicate with each other exclusively through discrete action potentials. For each parameter φ_l^i, we use the firing probability of neuron z_l^i to encode it. The WTA circuit G_l can satisfy the normalization condition for the parameters $\varphi_l^i(i=1,\ldots,K)$. Furthermore, we utilize the fact that a spiking train with EPSP kernel can be used to estimate fire probabilities of neurons in a nonparametric way [27]

$$I_l^i(t) \approx p_l^i(t) = \varphi_l^i(t).$$

In other words, each variational parameter φ_l^i is approximately represented by the spiking trains of the neuron z_l^i. Therefore, the dynamic firing equations (8) can be equivalent to mean field equations (22).

C. Variational Bayesian Learning Through STDP

We now establish a link between the STDP learning rule (11) and variational M-step. During the variational M-step, we derive the optimal updates to increase the lower bound $F(Q,\mathbf{w})$. Theorem 1 shows that the equilibrium points of the STDP rule (11) are equivalent to the optimal points of the lower bound $F(Q,\mathbf{w})$. In other words, the synaptic weights $\mathbf{w}$ over the STDP rule (11) will stochastically converge to the optimal points of variational M-step

$$\forall l,i,j: E_{\hat{p}}\Big[\Delta w_l^{ij}\Big] = 0 \Longleftrightarrow \frac{\partial\langle F(Q,\mathbf{w})\rangle_{p^*}}{\partial w_l^{ij}} = 0 \tag{23}$$

where $\hat{p}$ denotes the probability distribution $p^*(\mathbf{z_v})\cdot Q(z_h|\varphi)$.

Lemma 1: The equilibrium point of the STDP learning rule (11) is

$$\forall l,i,j: w_l^{ij} = \log\Big\langle S_l^i(t)S_{pa(l)}^j(t)\Big\rangle_{\hat{p}} - \log\Big\langle S_{pa(l)}^j(t)\Big\rangle_{\hat{p}}. \tag{24}$$

Proof:

$$\begin{aligned} &\forall i,l,j: E_{\hat{p}}\Big[\Delta w_l^{ij}\Big] = 0 \Longleftrightarrow \\ &e^{-w_l^{ij}}\Big\langle S_l^i(t)S_{pa(l)}^j(t)\Big\rangle_{\hat{p}}\int_0^\infty W(s)ds - \Big\langle S_{pa(l)}^i(t)\Big\rangle_{\hat{p}} = 0 \\ &\Longleftrightarrow e^{-w_l^{ij}}\Big\langle S_l^i(t)S_{pa(l)}^j(t)\Big\rangle_{\hat{p}} - \Big\langle S_{pa(l)}^i(t)\Big\rangle_{\hat{p}} = 0 \\ &\Longleftrightarrow w_l^{ij} = \log\Big\langle S_l^i(t)S_{pa(l)}^j(t)\Big\rangle_{\hat{p}} - \log\Big\langle S_{pa(l)}^j(t)\Big\rangle_{\hat{p}}. \end{aligned} \tag{25}$$

■

Theorem 1: The STDP learning rule (11) stochastically converges to the set of maxima of the lower bound of log-likelihood $F(Q,\mathbf{w})$ with probability one, subject to the normalization constraints

$$\forall l,j: Z_l^j = \sum_{i=1}^{K_l} e^{w_l^{ij}} = 1. \tag{26}$$

Proof: Since the weight synaptic updates $\Delta w_l^{ij}(\forall l,i,j)$ are random variables, the learning rule (14) is essentially a stochastic difference equation. According to the theory of stochastic approximation algorithms as presented in [34], the sequences $w_l^{ij}(t)(\forall l,i,j)$ stochastically convergence to the set of equilibrium points with probability one, where the learning rate $\xi_l^j(t)$ should obey the condition

$$\lim_{t\to\infty}\xi_l^j(t) = 0,\ \sum_{t=1}^{\infty}\xi_l^j(t) = \infty \text{ and } \sum_{t=1}^{\infty}\xi_l^j(t)^2 = 0. \tag{27}$$

It is easy to verify that the adaptive learning rate $\xi_l^j = (1/N_l^j)$ satisfies this condition. According to Lemma 1, the synaptic weight $w_l^{ij}(t)(\forall l,i,j)$ will convergence to equilibrium points (24). Therefore, we just need prove the equilibrium points are the optimal model parameters subject to the normalization constraints.

Setting the derivatives of the lower bound $\langle F(Q,\mathbf{w})\rangle_{p^*}$ to zero, we can get the following equations under the normalization constraints (26):

$$\begin{aligned}
&\forall i,l,j:\ \frac{\partial\langle F(Q,w)\rangle_{p^*}}{\partial w_l^{ij}}=0\\
&\Longleftrightarrow \frac{\partial\langle \log p(\mathbf{z}|\mathbf{w})\rangle}{\partial w_l^{ij}}=0\\
&\Longleftrightarrow \left\langle\delta\left(z_l=i,z_{pa(l)}=j\right)\right\rangle_{\hat{p}}-\frac{e^{w_l^{ij}}}{Z_l^j}\left\langle\delta\left(z_{pa(l)}=j\right)\right\rangle_{\hat{p}}=0\\
&\Longleftrightarrow \left\langle S_l^i(t)\cdot S_{pa(l)}^j(t)\right\rangle_{\hat{p}}-\frac{e^{w_l^{ij}}}{Z_l^j}\left\langle S_{pa(l)}^j(t)\right\rangle_{\hat{p}}=0\\
&\Longleftrightarrow \left\langle S_l^i(t)\cdot S_{pa(l)}^j(t)\right\rangle_{\hat{p}}-e^{w_l^{ij}}\left\langle S_{pa(l)}^j(t)\right\rangle_{\hat{p}}=0\\
&\Longleftrightarrow w_l^{ij}=\log\left\langle S_l^i(t)S_{pa(l)}^j(t)\right\rangle_{\hat{p}}-\log\left\langle S_{pa(l)}^j(t)\right\rangle_{\hat{p}}. \qquad (28)
\end{aligned}$$

■

Corollary 1: The intrinsic excitabilities $\{b_l^j|\forall l,j\}$ remain approximately constant under the STDP learning rule (11).

Proof: After the synaptic weights convergence to the equilibrium points, it is easily verified that

$$\begin{aligned}
&\forall\ l,j:\ \sum_{i=1}^{K(l)}\exp\left(w_l^{ij}\right)=1\Longrightarrow\\
&\forall\ l,j:\ b_l^j=-\sum_{c\in ch(l)}\sum_{i=1}^{K}e^{w_c^{ij}}=\text{constant}. \qquad (29)
\end{aligned}$$

Since there is always a stochastic fluctuation around the normalization conditions, the intrinsic excitabilities remain approximately constant.

Before the synaptic weights convergence to the equilibrium points, the intrinsic excitabilities are also roughly constant at each time step. We assume that the synaptic weights are initialized to satisfy the normalization constraints $\sum_{i=1}^{K}e^{w_l^{ij}(0)}=1$, then the $\sum_{i=1}^{K}e^{w_l^{ij}(t)}$ approximately equals to 1. Therefore, b_l^j is also approximately constant before convergence

$$\begin{aligned}
&\forall\ l,j:\\
&\sum_{i=1}^{K}\exp\left(w_l^{ij}(t)\right)\approx 1\Longrightarrow\\
&\sum_{i=1}^{K}\exp\left(w_l^{ij}(t+1)\right)=\sum_{i=1}^{K}\exp\left(w_l^{ij}(t)+\xi_l^j\triangle w_l^{ij}(t)\right)\\
&\approx\sum_{i=1}^{K}\exp\left(w_l^{ij}(t)\right)\left(1+\xi_l^j\triangle w_l^{ij}(t)\right)\\
&=\sum_{i=1}^{K}\exp\left(w_l^{ij}(t)\right)+\xi_l^j\sum_{i=1}^{K}\triangle w_l^{ij}(t)\\
&=\sum_{i=1}^{K}\exp\left(w_l^{ij}(t)\right)+\xi_l^jZ_l^j(t)\left(1-\sum_{i=1}^{K}\exp\left(w_l^{ij}(t)\right)\right)\\
&\approx 1. \qquad (30)
\end{aligned}$$

■

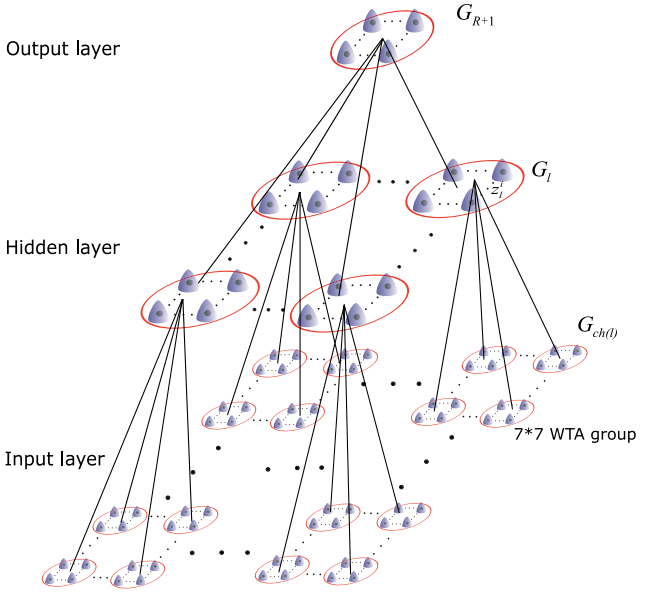

Fig. 5. Three layer hierarchical-WTA for MNIST experiment.

IV. Results

To validate our computational framework, we evaluate a three layer hierarchical-WTA on the MNIST benchmark. The MNIST dataset contains a training set of 60 000 examples and a test set of 10 000 examples. We show that the hierarchical-WTA can learn to discriminate handwritten digits from the MNIST dataset through spike-based variational EM algorithm without any supervision.

A. Network Architecture

The hierarchical-WTA used in the simulation is composed of three layers: 1) input; 2) hidden; and 3) output layer as shown in Fig. 5. The network has 801 WTA circuits in total. The input layer contains 28×28 WTA circuits $G_l, l=1,\ldots,784$ that has two excitatory neurons. WTA circuits of the input layer are used to encode the 28×28 pixel binarized digit images. Hidden layer contains 16 WTA circuits $G_l, l=785,\ldots,800$ consisting of K_h excitatory neurons. Each adjacent 7×7 WTA circuits of input layer are grouped as input to each WTA circuit of hidden layer in a feed-forward way (see Fig. 5). Output layer just has one WTA circuit denoted by G_{R+1}, where $R=800$. G_{801} is composed of K_o excitatory neurons. And this WTA circuit is connected to all the 16 WTA circuits of hidden layer. It should be noted that synaptic connections between hidden and output layer are bidirectional. In other words, the spiking neurons in the hidden layer can receive input from both output layer and input layer. G_{801} is the only WTA circuit of output layer and receive input from the hidden layer. Besides, each spiking neuron of G_{801} stands for a single classification of the digits.

Pixels of every digit image are binarized to 0 and 1 as preprocessing. Each pixel of the input image is encoded by each WTA circuit of input layer. (one spiking neuron represents 1 and the other represents 0). The binarized value is converted to Poisson-spike with firing rates 200 Hz of the

corresponding excitatory neuron, whereas the other neuron is inhibited and keeps silent. We present every digit image to the hierarchical-WTA network for 150 ms. In this way, 28×28 WTA circuits of input layer convert each digit image to Poisson-spike trains of 150 ms [see Fig. 7(a)]. Those spike trains are fed as forward input to spiking neurons of the hidden layer. Meanwhile, spiking neurons of the hidden layer also receive feedback input from the output layer. For example, as illustrated in Fig. 5, WTA circuit G_l receive feedforward input from input layer and backforward from output layer. And the spiking neurons of G_{801} receive input from all the spiking neurons of hidden layer. Then, the firing probability of all the spiking neurons of hidden and output layer is computed according to the dynamic firing equation (8).

B. Results

We first set $K_o = 100$ and $K_h = 15$, and consider the network with 100 output neurons and 16×15 hidden neurons. Of course, more networks with different scales of hidden and output neurons are also tested in the following section. We trained this network by presenting the entire training set of 60 000 examples. In the simulation, we use a discrete time step $\delta t = 1$ ms to update the dynamics of spiking neurons and synaptic weights. Each digit is presented for 150 ms. Thus the training process lasts 9000 s of biological time. The evolution of all synaptic weights is confined within a range $[0, w_{\max}]$. At the beginning of simulation, the synaptic weights of the network are randomly initialized. And initializations of the synaptic weights of the network need to be subject to the normalization constraints (26). During training, the firing activities of the hierarchical-WTA are decided by the dynamic firing equations (8) and the synaptic weight changes induced by the STDP learning rule (11). After training is done, we fix all the synaptic weights and test the network for the entire test of 10 000 examples. The predicted digit of each test example is determined by the highest average firing rate. We averages the responses of each output neuron and then choose the neuron with the highest firing rate as the predicted class of the test example. Then this network with 100 output neurons and 16×15 hidden neurons achieves average accuracy 82.75% over five experiments.

To display the effectiveness of our network, we compare outputs of the hierarchical WTA in response to the images before and after learning. We randomly select four handwritten digits $(0, 2, 6, 7)$ from the MNIST dataset. Each handwritten digit is encoded by 1568 spike trains over 500 ms. Color of spikes indicates the label of the handwritten digit, as illustrated in Fig. 7(a). Before learning, the spikes produced by the output neurons are completely random as shown in Fig. 7(b). In other words, the output neurons cannot classify the handwritten digits. After learning, we present the output spike trains in Fig. 7(c). Obviously, these 100 output neurons have self-organization for input stimuli so that four of output neurons specialize on the selected digit images.

In Fig. 7(d), we present the evolution curve of log-likelihood in the course of learning, which is averaging over five repetitions of the learning experiment. After convergence, the hierarchical-WTA gets an average -248 log-likelihood over five trails. As we can see, our spiking-based variational EM algorithm significantly enhances the networks learning capabilities. To demonstrate synaptic weights can convergence to the equilibrium points, we present two examples of synaptic weights that remove the shifted constant $\hat{w}$ as illustrated in Fig. 7(e) and (f). Fig. 7(e) shows the convergence curves of synaptic weights $w_{l=10}^{i,j=6}(i = 1, 2)$ that are synaptic connections between the WTA circuit $G_{l=10}$ in the input layer and the WTA circuit $G_{pa(l=10)}$ in the hidden layer. Fig. 7(f) shows the convergence curves of synaptic weights $w_{l=794}^{i,j=50}(i = 1, \ldots, 15)$ that are synaptic connections between the WTA circuit $G_{l=794}$ in the hidden layer and the WTA circuit G_{R+1} in the output layer.

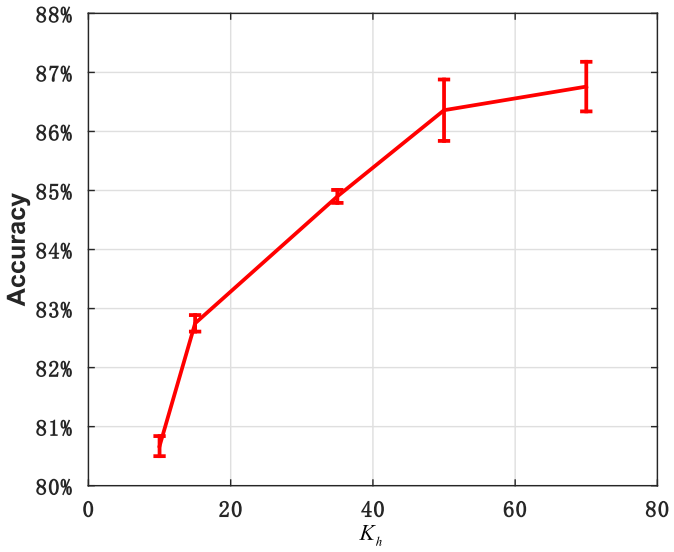

Fig. 6. Accuracy of networks of different scales of hidden neurons.

C. Experimental Comparison

1) Comparing With the Networks of Different Scales: To demonstrate the power of spike-based variational EM algorithm, we train and test the hierarchical-WTA networks with different scales of hidden neurons. We fix the number of output neurons to 100 ($K_o = 100$) and, respectively, set K_h to 10, 15, 35, 50, and 70. The network with 100 output neurons and 16×15 hidden neurons has been tested and achieved an average accuracy 82.75% over five experiments. Thus we need train and test the other networks on the MNIST dataset. Five hierarchical-WTA networks achieve 80.67%, 82.75%, 84.89%, 86.5%, and 86.76% average accuracy over five experiments. And the standard deviation is, respectively, 0.17%, 0.14%, 0.11%, 0.52%, and 0.42%. As illustrated in Fig. 6. the accuracy rate increases as K_h grows. K_h represents the number of states of hidden variables. To some degree, K_h decides the number of combination of abstract features that are presented to output layer. Thus, the bigger K_h is, the stronger the learning capacity of the network is. Of course, as K_h increases, the trend of performance will grow slowly or even decline, because of the existence of over fitting.

2) Comparing With Nessler et al. [22]: Nessler *et al.* [22] built a two layer spiking neural architecture

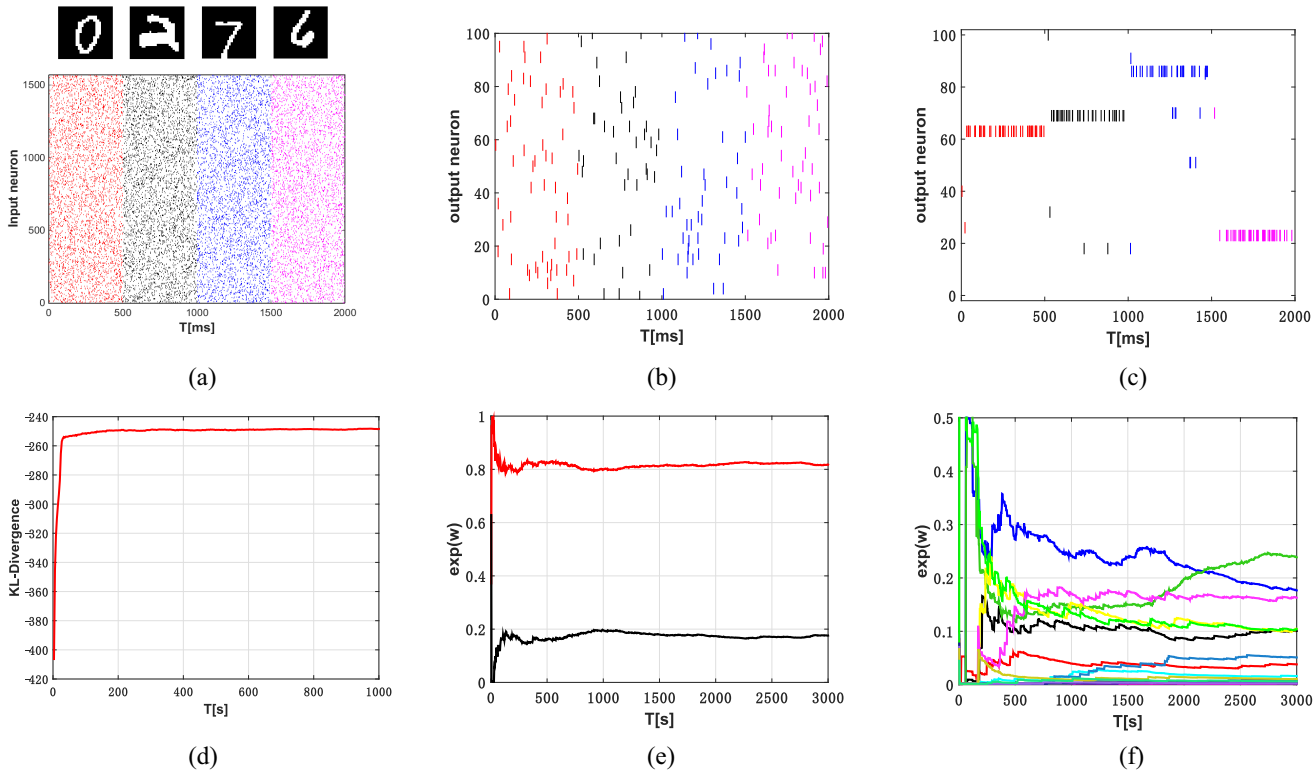

Fig. 7. (a) Input handwritten digit templates (digits 0, 2, 7, and 6) from MNIST database are represented by the spike trains from 784 WTA circuits including 1568 neurons. Response of the output WTA circuit given the four input templates (b) before training and (c) after training. (d) Convergence curve of log-likelihood function $L(\mathbf{w})$. Convergence curves of the synaptic weights (e) $\mathbf{w}_{l=10}^{i,j=6}(i=1,2)$ and (f) $\mathbf{w}_{l=794}^{i,j=50}(i=1,\ldots,15)$.

to perform inference and learning for the Bayesian model that just has a hidden node. They set the $K_o = 100$ neurons on the output layer and train the network on the MNIST training dataset in an unsupervised fashion. Their network achieves 80.14% accuracy over the unseen testset. In the case where the number of output neurons are 100, our network can reach up to 86.76% accuracy, which is much better than the performance of the method of Nessler *et al.* [22]. The underlying model in our framework is hierarchical Bayesian model, which has a stronger learning capacity than the Bayesian model that just has a hidden node. Thus our hierarchical-WTA obtains a higher accuracy.

3) Comparing With Diehl and Cook [35]: So far, the best result of unsupervised classification of digit recognition using spiking neural networks is acquired by Diehl and Cook [35]. They construct a two layer spiking neural network and train the networks with 100, 400, 1600, and 6400 output neurons on the MNIST benchmark. As shown in Table II, their four networks, respectively, achieve classification accuracy of 82.9%, 87.0%, 91.9%, and 95.0% on the test dataset. To compare with their work, we train four networks with the same sizes of output neurons. The number of hidden neurons is set to 35×16 (i.e., $K_h = 35$). Our networks achieve 84.89%±0.11%, 89.75%±0.19%, 92.23%±0.14%, and 95.0%±0.26% average classification accuracy over five experiments. This compares favorably to the accuracy that Nessler *et al.* [22] obtains. What is more, all of our networks are trained by presenting one times the training set. Nevertheless, their four networks are trained, respectively, by presenting 1, 3, 7, and 15 times the training set. On the other hand, compared with the networks of Diehl and Cook [35], hierarchical-WTA networks have larger standard deviation of the performance. Standard deviation of our four networks is, respectively, 0.11%, 0.19%, 0.14%, and 0.26%. The reason is that our networks have richer variability. In our framework, we treat spiking neuron as a stochastic model rather than the deterministic one. And the spiking neuron model used in the networks of Diehl and Cook [35] is deterministic leaky integrate-and-fire model. In fact, a intriguing idea is that biological neurons and synapses are both stochastic. Noise and trial-to-trial variability are not only treated as stochastic processes on the neural level, but also the computational strategy of the brain [36].

TABLE II
ACCURACY OF NETWORKS WITH DIFFERENT SCALES OF OUTPUT NEURONS

K_o	100	400	1600	6500
Ours ($K_h = 35$)	84.89%	89.75%	92.23%	95.0%
Diehl and Cook	82.9%	87.0%	91.9%	95.0%
Nessler et al.	80.14%	-	-	-

V. CONCLUSION

A. Significance and Novelty

Bayesian brain plays an important role in neuroscience and cognitive science. With the help of more and more related studies, we also have a profound understanding of how the brain performs Bayesian inference. However, much of the existing

work focus on neural implementations of simple probabilistic inference and the low-level perceptual problems such as cue combination and decision making [37]. The others study how Brain or cerebral cortex performs complex Bayesian inference in the view of macroscopic, such as the free-energy principle proposed by Friston [12] and the hierarchical Bayesian framework proposed by Lee and Mumford [11]. Therefore, there still remains a big gap between microscopic cortical circuits and the complex inference facing high-level cognitive problems. This paper actually aims at bridging this gap. We first propose that WTA circuits can be used to perform mean field inference, and then develop a spike-based variational EM algorithm based on STDP. This allow us to build neural network to implement the hierarchical Bayesian model. It is helpful to understand the processing of sensory stimuli from neural substrate to cognitive systems. Besides our network and algorithm can provide a versatile computational framework for novel neuromorphic hardware [38], [39].

B. Comparison

Several works try to explain how the brain implements hierarchical inference by various theories such as Monte Carlo sampling, predictive coding, and free-energy principle. Shi and Griffiths [13] built hierarchical networks of spiking neurons to implement hierarchical Bayesian inference by Monte Carlo sampling. They utilized one spiking neuron to represent one sample. However, the number of spiking neurons increases hugely as the number of hidden variables grows. Rao and Ballard [48] applied a hierarchical model of predictive coding to model the visual cortex processing. But their model of predictive coding is based on a linear model and hard to represent complex relationships of what caused its sensory input. Friston [12] proposed the free-energy principle as the global brain theory, which introduces the central role of Bayesian generative models and variational approaches to hierarchical inference and learning. While, his theory address explaining how the brain implements variational Bayesian inference in perspective of macroscopic.

In summary, Rao and Ballard's work is based on the theory of predictive coding. Friston's [12] work, Shi and Griffiths' [13] work, and this paper are based on the theory of Bayesian brain. The theme underlying these frameworks is that the brain is an inference machine. The most difference is that our algorithm is established in the cortical microcircuits and can explain how spiking neurons implement both hierarchical Bayesian inference and learning.

Recent, a number of spiking neural networks with biologically plausible learning rules have been developed for learning of MNIST classification. In summary, there are three types to train spiking neural networks including unsupervised, supervised, and reinforcement learning. To date, Diehl *et al.* [40] obtained the best performance (99.1%) on MNIST dataset by supervised learning. They train synaptic weights of the convolutional network by backpropagation and transfer those trained weights into a spiking neural network. Thus their network has nothing to do with STDP learning rules. Of course, there are STDP-based supervised algorithms. Beyeler *et al.* [41] used the STDP with teaching signals to train a multilayer spiking neural network and obtain 92% accuracy. Another approach is to train spiking neural network by reinforcement learning. Huerta and Nowotny [42] used the STDP with reward signals to train synaptic weights and achieve 93% accuracy on the MNIST test dataset. The other type is to train spiking neural network without any supervision. Our hierarchical-WTA can achieve 95% classification accuracy, which is quite to the network of Diehl and Cook [35]. So far, the best accuracy of unsupervised learning on MNIST is achieved by synaptic sampling machine [43]. Their network can reach up to 95.6% classification accuracy, which is slightly better than our hierarchical-WTA. However, in the framework of synaptic sampling machine, the synaptic update rule need a global modulatory signal. This modulatory signal is used to switch the behavior of synapse from LTP to LTD. Actually, whether synapse has such a behavior remains unknown. What is more, the sign of synaptic weights changes during the process of learning, which is not biologically plausible. Because it is impossible that synapses of neurons are both excitatory and inhibitory.

C. Future Work

Although our algorithm and results are meaningful and instructive, several important questions remain. First, the hierarchical-WTA is easy to perform the hierarchical Bayesian models with tree-like structure. For general networks, our strategy is converting an arbitrary Bayesian network to the one with tree-like structure by combining some variables together [24]. However, this strategy need enormous neurons to implement the Bayesian models with nontree structure. Because, the number of the states of the combined variable grows multiply and each state of the variable need a spiking neuron to represent. In the future work, we will directly extend our spike-based variational EM algorithm to the Bayesian models with nontree structure. Indeed, for Bayesian models in which nodes have many parents, mean field inference is also intractable [33]. Because it requires summing over an exponentially huge number of states of parents nodes. Thus, we need to do further approximation, such as quadratic bound approximation [33], Gaussian fields approximation [44], and so on. The core of following work is constructing more complex network of WTA circuits to implement approximate mean field inference. Second, generalizing our framework to continuous variables is also an important question, because most of input stimuli that the brain receives are continuous. The key to this question lies in how to represent the Bayesian models and variational distributions with continuous variables. Probabilistic population coding (PPC) [19] provides a biologically plausible representation scheme of probability distributions. We use a population of neurons directly to encode the variational distribution by PPC. And then we will drive the spike-based variational EM algorithm for the Bayesian models with continuous variables. Finally, the STDP rule (11) is unsupervised learning without teaching signals and it is also necessary to combine our framework with reinforcement learning or supervised learning. There is an increasing interest in synaptic plasticity rules

for reinforcement learning and supervised learning, such as reward-modulated STDP [45] and ReSuMe [46]. These learning rules mostly involve three factors including presynaptic activity, postsynaptic activity, and global modulated signals. The current opinion drawn from the physiological experiments suggests that this global signal can be dopamine [47]. For example, neurotransmitter from dopamine neurons in the substantia nigra functions as reward or supervisory signal, which is broadcast globally to brain areas. In the following, we will combine the STDP rule (11) with the global modulated signal and extend our algorithm to reinforcement learning or supervised learning.

REFERENCES

[1] A. Funamizu, B. Kuhn, and K. Doya, "Neural substrate of dynamic Bayesian inference in the cerebral cortex," *Nat. Neurosci.*, vol. 19, no. 12, pp. 1682–1689, 2016.

[2] K. P. Kording and D. M. Wolpert, "Bayesian integration in sensorimotor learning," *Nature*, vol. 427, no. 6971, pp. 244–247, 2004.

[3] M. O. Ernst and M. S. Banks, "Humans integrate visual and haptic information in a statistically optimal fashion," *Nature*, vol. 415, no. 6870, pp. 429–433, 2002.

[4] N. Chater, J. B. Tenenbaum, and A. Yuille, "Probabilistic models of cognition: Conceptual foundations," *Trends Cogn. Sci.*, vol. 10, no. 7, pp. 287–291, 2006.

[5] Z. Yu, F. Chen, J. Dong, and Q. Dai, "Sampling-based causal inference in cue combination and its neural implementation," *Neurocomputing*, vol. 175, pp. 155–165, Jan. 2016.

[6] J. M. Beck *et al.*, "Probabilistic population codes for Bayesian decision making," *Neuron*, vol. 60, no. 6, pp. 1142–1152, 2008.

[7] D. H. Hubel and T. N. Wiesel, "Shape and arrangement of columns in cat's striate cortex," *J. Physiol.*, vol. 165, no. 3, pp. 559–568, 1963.

[8] A. H. Bond, "An information-processing analysis of the functional architecture of the primate neocortex," *J. Theor. Biol.*, vol. 227, no. 1, pp. 51–79, 2004.

[9] L. Fontolan, B. Morillon, C. Liegeois-Chauvel, and A. L. Giraud, "The contribution of frequency-specific activity to hierarchical information processing in the human auditory cortex," *Nat. Commun.*, vol. 5, no. 5, p. 4694, 2014.

[10] H.-A. Jeon, "Hierarchical processing in the prefrontal cortex in a variety of cognitive domains," *Front. Syst. Neurosci.*, vol. 8, no. 8, p. 223, 2014.

[11] T. S. Lee and D. Mumford, "Hierarchical Bayesian inference in the visual cortex," *J. Opt. Soc. America A Opt. Image Sci. Vis.*, vol. 20, no. 7, pp. 1434–1448, 2003.

[12] K. Friston, "The free-energy principle: A unified brain theory?" *Nat. Rev. Neurosci.*, vol. 11, no. 2, pp. 127–138, 2010.

[13] L. Shi and T. L. Griffiths, "Neural implementation of hierarchical Bayesian inference by importance sampling," in *Proc. Adv. Neural Inf. Process. Syst.*, 2009, pp. 1669–1677.

[14] A. Nouri and H. Nikmehr, "Hierarchical Bayesian reservoir memory," in *Proc. 14th Int. CSI Comput. Conf. (CSICC)*, Tehran, Iran, 2009, pp. 582–587.

[15] Y. Lecun, Y. Bengio, and G. Hinton, "Deep learning," *Nature*, vol. 521, no. 7553, pp. 436–444, 2015.

[16] R. P. Rao, "Bayesian computation in recurrent neural circuits," *Neural Comput.*, vol. 16, no. 1, pp. 1–38, 2004.

[17] L. Buesing, J. Bill, B. Nessler, and W. Maass, "Neural dynamics as sampling: A model for stochastic computation in recurrent networks of spiking neurons," *PLoS Comput. Biol.*, vol. 7, no. 11, pp. 725–748, 2011.

[18] D. Pecevski, L. Buesing, and W. Maass, "Probabilistic inference in general graphical models through sampling in stochastic networks of spiking neurons," *PLoS Comput. Biol.*, vol. 7, no. 12, 2011, Art. no. e1002294.

[19] W. J. Ma, J. M. Beck, P. E. Latham, and A. Pouget, "Bayesian inference with probabilistic population codes," *Nat. Neurosci.*, vol. 9, no. 11, pp. 1432–1438, 2006.

[20] Y. Huang and R. P. N. Rao, "Bayesian inference and online learning in poisson neuronal networks," *Neural Comput.*, vol. 28, no. 8, pp. 1503–1526, 2016.

[21] P. Sountsov and P. Miller, "Spiking neuron network Helmholtz machine," *Front. Comput. Neurosci.*, vol. 9, no. 46, p. 46, 2015.

[22] B. Nessler, M. Pfeiffer, L. Buesing, and W. Maass, "Bayesian computation emerges in generic cortical microcircuits through spike-timing-dependent plasticity," *PLoS Comput. Biol.*, vol. 9, no. 4, 2013, Art. no. e1003037.

[23] D. Pecevski and W. Maass, "Learning probabilistic inference through spike-timing-dependent plasticity," *eNeuro*, vol. 3, no. 2, p. 0048, 2016.

[24] D. Koller and N. Friedman, *Probabilistic Graphical Models—Principles and Techniques*. Cambridge, MA, USA: MIT Press, 2009.

[25] M. Oster, R. Douglas, and S.-C. Liu, "Computation with spikes in a winner-take-all network," *Neural Comput.*, vol. 21, no. 9, pp. 2437–2465, 2009.

[26] D. Kappel, B. Nessler, and W. Maass, "STDP installs in winner-take-all circuits an online approximation to hidden Markov model learning," *PLoS Comput. Biol.*, vol. 10, no. 3, 2014, Art. no. e1003511.

[27] R. Naud, L. Paninski, W. Gerstner, and W. M. Kistler, *Neuronal Dynamics: From Single Neurons to Networks and Models of Cognition*. Cambridge, U.K.: Cambridge Univ. Press, 2014.

[28] S. Harmeling and C. K. I. Williams, "Greedy learning of binary latent trees," *IEEE Trans. Pattern Anal. Mach. Intell.*, vol. 33, no. 6, pp. 1087–1097, Jun. 2011.

[29] N. L. Zhang, "Hierarchical latent class models for cluster analysis," *J. Mach. Learn. Res.*, vol. 5, no. 6, pp. 697–723, 2004.

[30] R. P. Adams, Z. Ghahramani, and M. I. Jordan, "Tree-structured stick breaking for hierarchical data," in *Proc. NIPS*, Vancouver, BC, Canada, 2010, pp. 19–27.

[31] K. A. Heller and Z. Ghahramani, "Bayesian hierarchical clustering," in *Proc. 22nd Int. Conf. Mach. Learn.*, Bonn, Germany, 2005, pp. 297–304.

[32] C. M. Bishop, *Pattern Recognition and Machine Learning* (Information Science and Statistics). New York, NY, USA: Springer-Verlag, 2006.

[33] M. J. Wainwright and M. I. Jordan, "Graphical models, exponential families, and variational inference," *Found. Trends Mach. Learn.*, vol. 1, nos. 1–2, pp. 1–305, 2010.

[34] H. J. Kushner and G. G. Yin, "Stochastic approximation algorithms and applications," *J. Amer. Stat. Assoc.*, vol. 93, no. 443, pp. 763–766, 1997.

[35] P. U. Diehl and M. Cook, "Unsupervised learning of digit recognition using spike-timing-dependent plasticity," *Front. Comput. Neurosci.*, vol. 9, p. 99, Aug. 2015.

[36] W. Maass, "Noise as a resource for computation and learning in networks of spiking neurons," *Proc. IEEE*, vol. 102, no. 5, pp. 860–880, May 2014.

[37] D. E. Angelaki, Y. Gu, and G. C. DeAngelis, "Multisensory integration: Psychophysics, neurophysiology, and computation," *Current Opin. Neurobiol.*, vol. 19, no. 4, pp. 452–458, 2009.

[38] G. Indiveri, E. Chicca, and R. Douglas, "A VLSI array of low-power spiking neurons and bistable synapses with spike-timing dependent plasticity," *IEEE Trans. Neural Netw.*, vol. 17, no. 1, pp. 211–221, Jan. 2006.

[39] B. V. Benjamin *et al.*, "Neurogrid: A mixed-analog-digital multichip system for large-scale neural simulations," *Proc. IEEE*, vol. 102, no. 5, pp. 699–716, May 2014.

[40] P. U. Diehl *et al.*, "Fast-classifying, high-accuracy spiking deep networks through weight and threshold balancing," in *Proc. Int. Joint Conf. Neural Netw.*, 2015, pp. 1–8.

[41] M. Beyeler, N. D. Dutt, and J. L. Krichmar, "Categorization and decision-making in a neurobiologically plausible spiking network using a STDP-like learning rule," *Neural Netw.*, vol. 48, pp. 109–124, Dec. 2013.

[42] R. Huerta and T. Nowotny, "Fast and robust learning by reinforcement signals: Explorations in the insect brain," *Neural Comput.*, vol. 21, no. 8, pp. 2123–2151, 2009.

[43] E. O. Neftci, B. U. Pedroni, S. Joshi, M. Al-Shedivat, and G. Cauwenberghs, "Stochastic synapses enable efficient brain-inspired learning machines," *Front. Neurosci.*, vol. 10, no. 99, p. 241, 2016.

[44] D. Barber and P. Sollich, "Gaussian fields for approximate inference in layered sigmoid belief networks," in *Proc. Adv. Neural Inf. Process. Syst.*, 2000, pp. 393–399.

[45] R. Legenstein, D. Pecevski, and W. Maass, "A learning theory for reward-modulated spike-timing-dependent plasticity with application to biofeedback," *PLoS Comput. Biol.*, vol. 4, no. 10, 2008, Art. no. e1000180.

[46] F. Ponulak and A. Kasiński, "Supervised learning in spiking neural networks with resume: Sequence learning, classification, and spike shifting," *Neural Comput.*, vol. 22, no. 22, pp. 467–510, 2010.

[47] H. S. Seung, "Learning in spiking neural networks by reinforcement of stochastic synaptic transmission," *Neuron*, vol. 40, no. 6, pp. 1063–1073, 2003.

[48] R. P. N. Rao and D. H. Ballard, "Predictive coding in the visual cortex: A functional interpretation of some extra-classical receptive-field effects," *Nat. Neurosci.*, vol. 2, no. 1, pp. 79–87, 1999.

Shangqi Guo received the B.S. degree in mathematics and physics basic science from the University of Electronic Science and Technology of China, Chengdu, China, in 2015. He is currently pursuing the Ph.D. degree with the Department of Automation, Tsinghua University, Beijing, China.

His current research interests include inference in probabilistic graphical models, artificial intelligence, brain-inspired computing, and computational neuroscience.

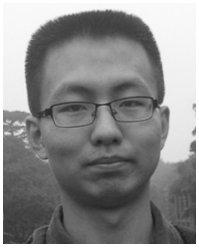

Zhaofei Yu received the B.S. degree from the College of Optoelectronic Engineering and the HongShen Honors School, Chongqing University, Chongqing, China, in 2012. He is currently pursuing the Ph.D. degree with the Department of Automation, Tsinghua University, Beijing, China.

His current research interests include inference in probabilistic graphical models, brain-inspired computing, and computational neuroscience.

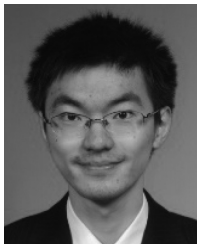

Fei Deng received the bachelor's degree in automation from Tsinghua University, Beijing, China, in 2015, where he is currently pursuing the master's degree in control science and engineering.

His current research interests include computer vision, deep learning, reinforcement learning, and brain-inspired computing.

Xiaolin Hu (S'01–M'08–SM'13) received the B.E. and M.E. degrees in automotive engineering from the Wuhan University of Technology, Wuhan, China, in 2001 and 2004, respectively, and the Ph.D. degree in automation and computer-aided engineering from the Chinese University of Hong Kong, Hong Kong, in 2007.

He is currently an Associate Professor with the Department of Computer Science and Technology, Tsinghua University, Beijing, China. His current research interests include artificial neural networks, computer vision, and computational neuroscience.

Dr. Hu is an Associate Editor of the IEEE TRANSACTIONS ON NEURAL NETWORKS AND LEARNING SYSTEMS.

Feng Chen (M'06) received the B.S. and M.S. degrees in automation from Saint-Petersburg Polytechnic University, Saint Petersburg, Russia, in 1994 and 1996, respectively, and the Ph.D. degree from the Automation Department, Tsinghua University, Beijing, China, in 2000.

He is currently a Professor with Tsinghua University. His current research interests include computer vision, brain-inspired computing, and inference in graphical models.